

# Accumulation of Phosphorylated Repressor for Gibberellin Signaling in an F-box Mutant

Akie Sasaki,<sup>1\*</sup> Hironori Itoh,<sup>1\*</sup> Kenji Gomi,<sup>1</sup> Miyako Ueguchi-Tanaka,<sup>1</sup> Kanako Ishiyama,<sup>2</sup> Masatomo Kobayashi,<sup>2</sup> Dong-Hoon Jeong,<sup>3</sup> Gynheung An,<sup>3</sup> Hidemi Kitano,<sup>4</sup> Motoyuki Ashikari,<sup>1</sup> Makoto Matsuoka<sup>1†</sup>

Gibberellin (GA) regulates growth and development in plants. We isolated and characterized a rice GA-insensitive dwarf mutant, *gid2*. The *GID2* gene encodes a putative F-box protein, which interacted with the rice Skp1 homolog in a yeast two-hybrid assay. In *gid2*, a repressor for GA signaling, SLR1, was highly accumulated in a phosphorylated form and GA increased its concentration, whereas SLR1 was rapidly degraded by GA through ubiquitination in the wild type. We conclude that GID2 is a positive regulator of GA signaling and that regulated degradation of SLR1 is initiated through GA-dependent phosphorylation and finalized by an SCF<sup>GID2</sup>-proteasome pathway.

Gibberellins (GAs) are essential regulators of diverse growth and developmental processes in plants (1). Recently, a constitutive GA response mutant, *slender rice1* (*slr1*) (Fig. 1A), was isolated and molecular biological analyses revealed that the *SLR1* gene encodes a protein orthologous to *Arabidopsis* GAI and RGA, wheat Rht, maize d8, and barley SLN1 (2–6). Using the *Arabidopsis gai* mutant, Peng *et al.* (2) proposed that GA signaling is governed by derepression of a repressor protein, GAI. This idea has been substantiated by recent studies on RGA, SLR1, and SLN1; that is, these proteins function in nuclei and degrade rapidly when exposed to GA, enabling the GA signal to be transmitted downstream (7–10). More recently, Fu *et al.* (11) indicated that proteasome-dependent degradation is necessary for GA-mediated destabilization of SLN1. How GA triggers the proteasome-mediated degradation of these repressor proteins remains unknown.

To investigate the molecular mechanism of GA signaling, we isolated several candidates showing a severe dwarf phenotype (12). Genetic analyses of these candidates revealed that the dwarf phenotype was inherited in a recessive manner and could be categorized in two groups: GA-insensitive dwarf 1 and 2 (*gid1* and -2). Here, we report that the GA-insensitive phenotype of *gid2* is caused by the

loss of function of a putative F-box protein.

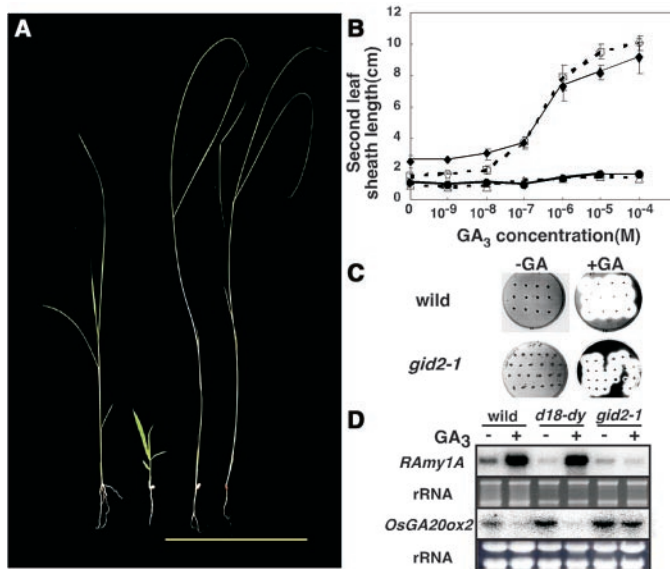
The *gid2* mutant showed a severe dwarf phenotype with wide leaf blades and dark green leaves (Fig. 1A), features typical of GA-related mutants such as *d1* and *d18* (13, 14). The *gid2-1/slr1-1* double mutants showed a slender phenotype identical to that of the *slr1-1* single mutant (Fig. 1A), indicating that GID2 functions upstream of SLR1. To confirm that *gid2* was a GA-insensitive mutant, we compared the GA responsiveness of *gid2-1* and *gid2-2* with that of the wild type and a GA-deficient mutant, *d18-dy*. When we treated the second leaf sheaths of these plants with various concentrations of

GA<sub>3</sub>, the wild type and *d18-dy* elongated at GA<sub>3</sub> concentrations of 10 nM or higher, whereas we observed very little response in both *gid2* mutants (Fig. 1B). We also examined the induction of α-amylase by GA<sub>3</sub> in *gid2-1* endosperm (Fig. 1C). α-Amylase activity was induced in all wild-type embryoless half seeds by GA treatment. However, GA did not induce α-amylase activity in 25% of the embryoless half seeds derived from *gid2-1* heterozygous plants. We observed no GA-dependent induction of α-amylase in *gid2-1* at the transcriptional level (Fig. 1D).

We also examined GA biosynthesis in *gid2-1*. First, we analyzed the expression of the GA20-oxidase gene, *OsGA20ox2*, which is highly expressed in vegetative organs (15). In the wild type and in *d18-dy*, *OsGA20ox2* expression was suppressed by GA<sub>3</sub> treatment, corresponding to feedback regulation of GA biosynthetic genes by bioactive GAs (Fig. 1D). However, GA<sub>3</sub> treatment did not suppress *OsGA20ox2* expression in *gid2-1*. We also directly measured the GAs in *gid2-1* and wild type. The amount of GA<sub>1</sub>, the dominant bioactive GA in rice vegetative organs, in *gid2-1* was more than 100 times higher than that detected in wild type (Table 1). Taken together, these results demonstrate that *gid2* is a GA-insensitive mutant and the *GID2* gene encodes a positive regulator of GA signaling.

To elucidate the molecular function of *GID2*, we isolated the gene by positional cloning. Because *gid2* was sterile, we crossed a japonica variety of *GID2/gid2* rice with an indica rice variety (Kasalath) and selected F<sub>1</sub> plants with a *GID2/gid2* genotype. About 2500 F<sub>2</sub> plants derived from these heterozygous F<sub>1</sub> plants were used in this study. The candidate

**Fig. 1.** Phenotype of the *gid2* mutant. (A) Gross morphologies of wild type, *gid2-1*, *gid2-1/slr1-1*, and *slr1-1* plants (left to right) in 2-week-old seedlings. Bar = 10 cm. (B) Elongation of the second leaf sheath in response to GA<sub>3</sub> treatment in *gid2-1* (●), *gid2-2* (Δ), *d18-dy* (○), and wild-type (◆) plants. Error bars represent standard deviation from the mean (n = 5). (C) α-Amylase induction in embryoless half seeds of the wild type and *gid2-1*. Embryoless half seeds from wild-type or *gid2-1* heterozygous plants were placed on starch plates with (+) or without (–) 1 μM GA<sub>3</sub>. Starch was detected by staining with iodine. (D) Effect of GA<sub>3</sub> on expression of α-amylase (*RAmy1A*) and *OsGA20ox2* in wild type, *d18-dy*, and *gid2-1*. The gel was stained with ethidium bromide as a control (rRNA) (13).



<sup>1</sup>BioScience Center, Nagoya University, Nagoya 464-8601, Japan. <sup>2</sup>BioResources Center, Riken, Tsukuba 305-0074, Japan. <sup>3</sup>Division of Molecular and Life Science, Pohang University of Science and Technology, Pohang 790-784, Republic of Korea. <sup>4</sup>Graduate School of Bioagricultural Science, Nagoya University, Nagoya 464-8601, Japan.

\*These authors contributed equally to this work. †To whom correspondence should be addressed. E-mail: makoto@agr.nagoya-u.ac.jp

region was narrowed down to a 13-kb sequence containing three putative genes. We compared this 13-kb sequence in the wild type with the corresponding region in the three *gid2* mutants and found nucleotide substitution or deletions in one predicted gene (Fig. 2A). The deletions

or substitution of nucleotide in all three *gid2* alleles introduced a novel stop codon, suggesting that these are null alleles. Introduction of a 4.2-kb *Sac* I fragment covering the entire region of the *GID2* gene in the *gid2-1* plants recovered the normal phenotype, confirming that the *gid2*

mutation is caused by a defect in *GID2* (16).

The *GID2* gene encoded a 639-base-pair open reading frame capable of producing a polypeptide of 212 amino acid residues (Fig. 2A). The deduced amino acid sequence of *GID2* contained an F-box domain, which is a conserved motif of F-box proteins that form part of an E3 ubiquitin-ligase complex. The motif found in *GID2* is well conserved in other F-box proteins, with the greatest similarity to *Arabidopsis* SLY1, which is a positive regulator of GA signaling (Fig. 2B) (17).

To confirm that *GID2* actually encodes an F-box protein, we examined whether *GID2* interacts with rice orthologs of Skp1 by a yeast two-hybrid analysis. F-box protein functions as a component of the SCF complex through interaction with Skp1 (18, 19). Thus, if *GID2* functions as an F-box protein, it will interact with a suitable Skp1 protein. We isolated 14 homologous genes from rice, designated *Os-Skp1-14* (*Oryza sativa* Skp1 homolog 1-14). We tested the interaction between *GID2* and two rice Skp1 candidates (*OsSkp2* and *OsSkp5*) because these two proteins showed high similarity to *Arabidopsis* ASK1 (fig. S1) (20). *GID2* interacted with *OsSkp2* to produce a blue colony, whereas a combination of *GID2* and *OsSkp5* did not induce lacZ activity (Fig. 2C). This indicates that *GID2* preferentially interacts with one or more members of Skp1 proteins.

As already noted, the SLR1 protein functions as a repressor of GA signaling in rice and its degradation may be essential for downstream action of GA. We examined whether this is also the case in the *gid2* mutant by probing immunoblots with an antibody to SLR1 (Fig. 3A). The SLR1 protein was abundant in *gid2-1* but was detected at a very low level in the wild type (compare lanes 1 and 3). Further, GA-dependent degradation of the SLR1 protein occurred in the wild type but was not observed in *gid2-1* (Fig. 3A). In addition, the immunoreactive protein in the *gid2* mutant was split into two bands, but only one band was detected in the wild type (Fig. 3A). The band in *gid2-1* with higher mobility corresponded to the protein synthesized in *Escherichia coli*—namely, the nascent protein (Fig. 3A); the band with lower mobility may be an intermediate in the SLR1 degradation process. The high level accumulation of SLR1 and the appearance of a new band with lower mobility in *gid2* suggest that GA-dependent degradation of SLR1 is deficient in *gid2*.

To investigate the nature of the modification in the SLR1 protein, we treated a crude extract of *gid2-1* with calf intestine alkaline phosphatase (CIP) before immunoblotting (Fig. 3B). This treatment caused the band with lower mobility in *gid2-1* to disappear, suggesting that this band comprises a phosphorylated form of the SLR1 protein. We also examined phosphorylation of the SLR1 protein by in vivo labeling with  $^{32}\text{PO}_4^-$ . Because we predicted that GA would enhance the degradation of the phospho-

**Fig. 2.** Sequence analyses and molecular characterization of *GID2*. (A) The *GID2* gene consists of one exon encoding an F-box motif (thick line). Nucleotide deletions (thin lines) and substitution (at the site of 618) in the three *gid2* alleles are represented. Black and shadow boxes indicate the coding and 5'- or 3'-flanking regions, respectively. (B) Alignment of the F-box motif of *GID2* with other F-box proteins (26): *GID2* (rice, accession number AB100246), SLY1 (*Arabidopsis*, accession number CAB45056), MET30 (yeast, accession number P39014), POF1 (*Schizosaccharomyces*, accession number P87053), SCON2 (mold, accession number Q01277), 1FQV A (human, accession number 1FQVA), FBX8 (human, accession number AAF04517), FBX22 (human, accession number AAF045223), and FBX29 (human, accession number AAF03129). Dark and light shading indicate identical and similar residues, respectively. (C) Interaction between *GID2* and *OsSkps* in a yeast two-hybrid assay. For bait construct (BD-*GID2*), full-length *GID2* was fused with the GAL4 DNA binding domain. For the prey constructs (AD-fusion), full-length *OsSkp2* or *OsSkp5* was fused with the GAL4 transcriptional activation domain (13).

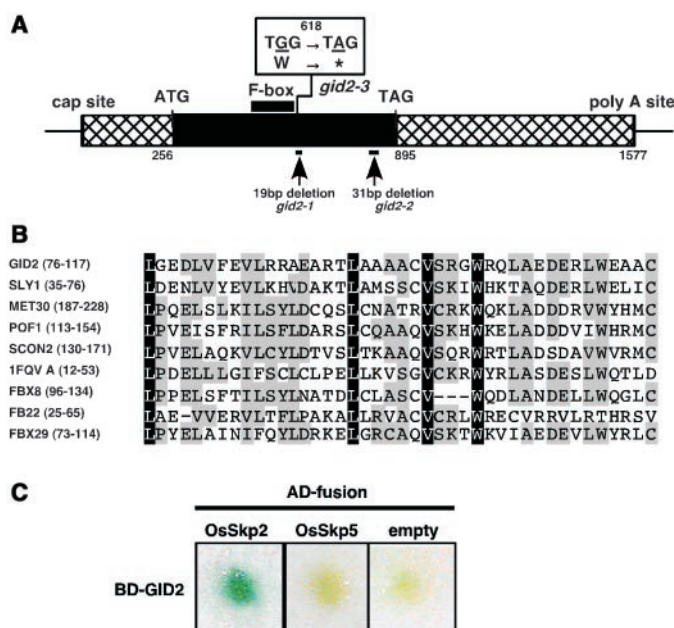
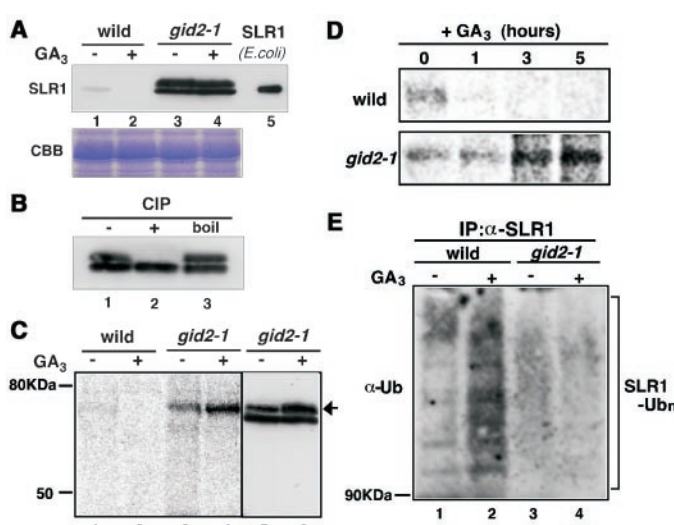


**Fig. 3.** Accumulation of the phosphorylated SLR1 protein in *gid2*. (A) Immunoblotting of SLR1 was done with 10  $\mu\text{g}$  of protein of crude extract from wild type (lanes 1 and 2) and *gid2-1* (lanes 3 and 4) treated with (+) or without (-) 100  $\mu\text{M}$   $\text{GA}_3$ . Recombinant SLR1 produced in *E. coli* was used as a size control (lane 5), and the Coomassie brilliant blue-stained RbcS protein was used as a loading control (CBB). (B) A crude extract of *gid2-1* was incubated with (+) or without (-) CIP. Boiled CIP was used as a negative control (boil). (C and D) In vivo phosphorylation of the SLR1 protein. Seedlings of wild type or *gid2-1* pretreated with 1  $\mu\text{M}$  uniconazole were incubated with  $^{32}\text{PO}_4^-$  and then treated with (+) or without (-) 100  $\mu\text{M}$   $\text{GA}_3$  for 2 hours in (C) or collected with a time course following the  $\text{GA}_3$  treatment in (D). Proteins immunoprecipitated with the antibody to SLR1 were analyzed by autoradiography [lanes 1 to 4 in (C) and (D)] or immunoblotting with the antibody to SLR1 [lanes 5 and 6 in (C)]. (E) Detection of the polyubiquitinated SLR1 in wild type and *gid2-1*. Seedlings were pretreated with the proteasome inhibitor MG132 before  $\text{GA}_3$  treatment. One milligram of total protein extract was immunoprecipitated with antibody to SLR1 (IP:  $\alpha$ -SLR1) and analyzed by immunoblotting with antibody to Ub ( $\alpha$ -Ub) (13).



## REPORTS

**Table 1.** Amounts of endogenous GAs in wild type and *gid2* (ng per g of fresh weight).

	GA <sub>53</sub>	GA <sub>44</sub>	GA <sub>19</sub>	GA <sub>20</sub>	GA <sub>1</sub>
Wild type					
Lot 1	5.6	2.6	20	0.5	0.3
Lot 2	4.0	2.9	28	0.3	0.5
<i>gid2-1</i>					
Lot 1	4.1	6.0	26	2.4	47
Lot 2	4.2	6.0	23	2.4	56

rylated SLR1 protein, we pretreated the wild type and *gid2-1* with uniconazol, an inhibitor of GA biosynthesis. We detected one faint radioactive band in uniconazol-pretreated wild type and this band disappeared after treatment with GA<sub>3</sub> (Fig. 3C, lanes 1 and 2). This supports our theory that the phosphorylated SLR1 protein is destabilized by bioactive GA. In contrast, we observed one strong radioactive band in *gid2-1* and GA<sub>3</sub> treatment increased its intensity (Fig. 3C, lanes 3 and 4). The mobility of the radioactive band corresponded to the upper band in *gid2-1*, and the intensity of the upper band observed by immunoblotting increased after treatment with GA (Fig. 3C, lanes 5 and 6). This GA-induced phosphorylation of SLR1 protein in *gid2-1* was gradually increased after GA<sub>3</sub> treatment (Fig. 3D). These results indicate that GA increases SLR1 phosphorylation and may lead to degradation of phosphorylated SLR1 in wild type but that degradation of the phosphorylated SLR1 in *gid2* is inhibited and consequently the protein is accumulated.

The fact that a loss of function in an F-box protein, GID2, causes accumulation of the SLR1 protein leads us to speculate that GA-dependent degradation of SLR1 protein is caused by the ubiquitin/26S proteasome pathway. To test this possibility, we examined the polyubiquitination of SLR1 protein in vivo by immunoblotting with antibody to ubiquitin (Ub). In wild type treated with a proteasome inhibitor, MG132, a low level of polyubiquitinated SLR1 was observed without GA treatment (Fig. 3E, lane 1), and GA treatment induced the accumulation of polyubiquitinated SLR1 protein (Fig. 3E, lane 2). In contrast, in *gid2-1*, we observed no ubiquitinated SLR1 with or without GA treatment (Fig. 3E, lanes 3 and 4). These results suggest that the SLR1 protein is degraded via the ubiquitin/26S proteasome pathway mediated by the SCF<sup>GID2</sup> complex.

The F-box protein in the SCF complex functions as a receptor that selectively recruits target proteins into the complex to degrade these proteins through ubiquitination. This SCF-mediated signaling pathway is well conserved in yeast, mammals, and higher plants (21–25). According to recent advances in understanding SCF-mediated pathways in yeast and animals (21–23), modification of the target protein is a prerequisite for interaction between the target and F-box proteins, and phosphorylation is one of the most common types of modification of target proteins. Although there are no previous

reports that phosphorylation of target proteins triggers SCF-mediated degradation in plants, our results indicate that GA-dependent phosphorylation of SLR1 triggers the ubiquitin-mediated degradation in a manner similar to the SCF-mediated pathway in yeast and animals.

### References and Notes

- P. J. Davies, *Plant Hormones* (Kluwer Academic, Dordrecht, Netherlands, 1995).
- J. Peng *et al.*, *Genes Dev.* **11**, 3194 (1997).
- A. L. Silverstone, C. N. Ciampaglio, T.-P. Sun, *Plant Cell* **10**, 155 (1998).
- J. Peng *et al.*, *Nature* **400**, 256 (1999).
- A. Ikeda *et al.*, *Plant Cell* **13**, 999 (2001).
- P. M. Chandler, A. Marion-Poll, M. Ellis, F. Gubler, *Plant Physiol.* **129**, 181 (2002).
- A. L. Silverstone *et al.*, *Plant Cell* **13**, 1555 (2001).
- A. Dill, H.-S. Jung, T.-P. Sun, *Proc. Natl. Acad. Sci. U.S.A.* **98**, 14162 (2001).
- H. Itoh, M. Ueguchi-Tanaka, Y. Sato, M. Ashikari, M. Matsuoka, *Plant Cell* **14**, 57 (2002).
- F. Gubler, P. M. Chandler, R. G. White, D. J. Llewellyn, J. V. Jacobsen, *Plant Physiol.* **129**, 191 (2002).
- X. Fu *et al.*, *Plant Cell* **14**, 3191 (2002).

- Materials and methods are available as supporting material on Science Online.
- M. Ashikari, J. Wu, M. Yano, T. Sasaki, A. Yoshimura, *Proc. Natl. Acad. Sci. U.S.A.* **96**, 10284 (1999).
- H. Itoh *et al.*, *Proc. Natl. Acad. Sci. U.S.A.* **98**, 8909 (2001).
- M. Ashikari *et al.*, *Breed. Sci.* **52**, 143 (2002).
- A. Sasaki *et al.*, data not shown.
- C. M. Steber, S. E. Cooney, P. McCourt, *Genetics* **149**, 509 (1998).
- E. T. Kipreos, M. Pagano, *Genome Biol.* **5**, 1 (2000).
- R. J. Dashaies, *Annu. Rev. Cell Dev. Biol.* **15**, 435 (1999).
- M. Yang *et al.*, *Proc. Natl. Acad. Sci. U.S.A.* **96**, 11416 (1999).
- F. N. Li, M. Jonston, *EMBO J.* **16**, 5629 (1997).
- D. Skowrya, K. L. Craig, H. Tyers, S. J. Elledge, J. W. Harper, *Cell* **91**, 209 (1997).
- J. T. Winston *et al.*, *Genes Dev.* **13**, 270 (1999).
- W. M. Gray, S. Kepinski, D. Rouse, O. Leyser, M. Estelle, *Nature* **414**, 271 (2001).
- L. Xu *et al.*, *Plant Cell* **14**, 1999 (2002).
- Single-letter abbreviations for the amino acid residues are as follows: A, Ala; C, Cys; D, Asp; E, Glu; F, Phe; G, Gly; H, His; I, Ile; K, Lys; L, Leu; M, Met; N, Asn; P, Pro; Q, Gln; R, Arg; S, Ser; T, Thr; V, Val; W, Trp; and Y, Tyr.
- We thank C. Steber for sharing SLY1 data prior to publication, A. Yoshimura for donating the rice dwarf mutant stock, and S. Hattori for excellent technical assistance. Supported by a Grant-in-Aid for the Center of Excellence, a Grant-in-Aid from the Program for the Promotion of Basic Research Activities for Innovative Bioscience (M.M.), the MAFF Rice Genome Project (M.A., M.M.), and a research fellowship from Japan Society for the Promotion of Science (H.I.).

### Supporting Online Material

www.sciencemag.org/cgi/content/full/299/5614/1896/DC1

Materials and Methods

Fig. S1

References

3 December 2002; accepted 22 January 2003

# Discrete Coding of Reward Probability and Uncertainty by Dopamine Neurons

Christopher D. Fiorillo,\* Philippe N. Tobler, Wolfram Schultz

Uncertainty is critical in the measure of information and in assessing the accuracy of predictions. It is determined by probability  $P$ , being maximal at  $P = 0.5$  and decreasing at higher and lower probabilities. Using distinct stimuli to indicate the probability of reward, we found that the phasic activation of dopamine neurons varied monotonically across the full range of probabilities, supporting past claims that this response codes the discrepancy between predicted and actual reward. In contrast, a previously unobserved response co-varied with uncertainty and consisted of a gradual increase in activity until the potential time of reward. The coding of uncertainty suggests a possible role for dopamine signals in attention-based learning and risk-taking behavior.

The brain continuously makes predictions and compares outcomes (or inputs) with those predictions (1–4). Predictions are fundamentally concerned with the probability that an event will occur within a specified time period. It is only through a rich representation of probabilities that an animal can infer the structure of its environment and form associations between correlated events (4–7). Substantial evidence indicates that do-

pamine neurons of the primate ventral mid-brain code errors in the prediction of reward (8–10). In the simplified case in which reward magnitude and timing are held constant, prediction error is the discrepancy between the probability  $P$  with which reward is predicted and the actual outcome (reward or no reward). Thus, if dopamine neurons code reward prediction error, their activation after reward should decline monotonically as the